Applied Biochemistry and Biotechnology
https://doi.org/10.1007/s12010-024-05022-1

ORIGINAL ARTICLE

Integration of RCA-Based DNA Nanoscaffold with Target Triggered RNA-Cleaving DNAzyme for Sensitive Detection of miRNA21

Yuan Li[1] · Xuefei Lv[1] · Hao Jiang[1] · Xiaoqiong Li[1] · Yulin Deng[1]

Accepted: 23 July 2024

Abstract
Cascaded amplification showed promising potential for detection of trace target miRNAs in molecular diagnosis and prevention of many diseases. In this study, miRNA21 was chosen as the target, and rolling circle amplification (RCA)-based DNA nanoscaffold was integrated with target triggered RNA-cleaving DNAzyme for sensitive detection of miRNA21. That is, the H1 probe was bound with the long-chain product of RCA to self-assemble into DNA nanoscaffold. Target miRNA21 triggered the hybridization chain reaction (HCR) located on the nanoscaffold, and led to rapid proximity of DNAzyme fragments modified at both ends of the H2 probe, which realized the cyclic cleavage of self-quenching substrate probe efficiently, and the fluorescence signal was restored. The results demonstrated that the proposed assay was sensitive, 0.76 pM of miRNA21 can be detected. The proposed assay was specific; only one-base mismatched miRNA21 can be effectively recognized, other nucleic acid sequence and the serum matrix did not cause any interference. The proposed assay was accurate; recoveries from 82.1 to 115.0% can be obtained in the spiked fetal bovine serum (FBS). The flexible and programmable characteristics of DNA nanoscaffold and DNAzyme provide a confident and robust strategy for more sensitive nucleic acid detection, and can be developed to be a universal sensing platform for detecting other miRNAs just needing modification on the corresponding sequence of H1 probe in HCR.

Keywords MiRNA · DNA nanoscaffold · DNAzyme · Isothermal cascaded amplification · RCA · HCR · Sensitive detection

Introduction

MiRNAs have been widely found in various animal and plant cells, and play a key role in various biological activities, for example, proliferation, differentiation, and apoptosis [1–3]. It has been demonstrated that thousands of miRNAs regulated gene expression at

✉ Xuefei Lv
xuefeilv@163.com

[1] Beijing Key Laboratory for Separation and Analysis in Biomedicine and Pharmaceuticals, School of Medical Technology, Beijing Institute of Technology, Beijing 100081, China

the post-transcriptional level. MiRNA participates in various regulatory pathways such as hematopoiesis and lipid metabolism [4, 5], and is closely related to the diagnosis, treatment, and prognosis of various tumor diseases, hematopoietic damage, and other medical diseases [6, 7]. It has become a new and highly promising biomarker for disease diagnosis [8, 9]. Thus, more and more attention has been paid to developing various methods for miRNA detection.

Polymerase chain reaction (PCR) and its derivative technology digital PCR (dPCR) have high sensitivity and accuracy for miRNA detection, but they require tedious cDNA synthesis and primer design [10–12]. With in-depth development of a series of nucleic acid isothermal amplification techniques, revolutionary changes have been made in the field of nucleic acid detection dominated by PCR. Compared with PCR, isothermal amplification techniques significantly improved detection speed, reduced reagent cost, avoided precise instruments, and realized exponential amplification with a simple constant temperature incubation equipment [13–15].

The isothermal amplification techniques can be mainly divided into enzyme-mediated and enzyme-free isothermal amplification techniques. Rolling circle amplification (RCA) is a representative enzyme-mediated nucleic acid isothermal amplification technique, which is established based on the rolling circle replication in nature. Complete complementarity between the probe and the primer is necessary for RCA, which produces high specificity and can even identify single base alteration [16]. However, RCA commonly uses the target as a primer, which somewhat hampers the development of its sensitivity [17]. Hybrid chain reaction (HCR) is a representative enzyme-free isothermal amplification technique, which possesses good environmental adaptability and easy operation [18], and have been widely used in miRNA amplification and detection [19]. Unfortunately, HCR is a chemical equilibrium-based amplification method; its efficiency is still unsatisfactory compared with that of enzyme-based amplification techniques.

In order to satisfy the requirement for trace contents of target nucleic acid detection, several isothermal amplification techniques were cascaded by using the product of the previous round of amplification as the trigger for the subsequent round of amplification to further improve the sensitivity and efficiency. For example, RCA was cascaded with loop-mediated isothermal amplification (LAMP) to detect miRNA let 7a with the detection limit as low as 0.12 fM [20]. Catalytic hairpin assembly reaction (CHA) was combined with HCR for miRNA-21 detection, and boost sensitivity in comparison to a single amplification by 5 orders of magnitude was realized [21]. However, some problems are still remained to be solved in cascaded isothermal amplification techniques, for example, the number of levels affects the amounts of amplification products accumulating in each layer, and the coexistence of multiple probes in solution might cause instability. Therefore, it is urgent to develop new cascade amplification technique-based universal methods for simple, specific, accurate, and sensitive miRNA detection.

As for detecting the amplified products of cascaded amplification techniques, a variety of methods have been developed, including electrochemical [22, 23], colorimetric [24], and fluorescent methods [25], and so on. In recent years, more attention has been paid to DNAzyme, which can be functioned as a tool for fluorescence signal generation. DNAzyme is fundamentally a nucleic acid and is stable and easy to be synthesized under a variety of environmental conditions. It performs the function of catalyzing the chemical processes of DNA breakage and oxidation [26]. More importantly, the sequence of DNAzyme can be designed and altered as necessary to match with various detection targets [27]. Until now, a variety of DNAzyme-based biosensor have been developed for the detection of small molecules [28, 29], proteins [30, 31], and viruses [32, 33]. It is certain that DNAzyme coupled

with cascaded amplification technique can play an important role in enhancing the detection performance.

In this study, miRNA 21 was chosen as the target. Most of the available evidence shows that the expression of miRNA 21 is maintained through transcriptional and post transcriptional regulation, thus participating in the pathogenesis of diseases [34]. miRNA21 also appears to be regulated in the expression of various cancer genes, such as breast cancer [35] and liver cancer [36], and it is considered to be an anti-apoptotic factor for cancer gene expression. Until now, various methods based on isothermal amplification techniques have been developed for miRNA 21 detection. For example, Wang et al. developed a detection platform for miRNA21 based on hyperbranching chain reaction with the detection limit of 2.14 pM [37]. MiRNA21 was also detected by integration CHA with HCR with a detection limit of 4 pM, and the reaction time was 5 h [38]. It can be found that there is still room for improvement in the probe design, the experimental operation, and the detection sensitivity. This study aims to develop a cascaded amplification technique-based platform for miRNA21 detection with high sensitivity, high accuracy, and high specificity, without complex probes design and complex experimental operations. In this strategy, the amplified product of RCA was used as the DNA nanoscaffold, HCR-formed complete DNAzyme was used for signal generation. In the presence of miRNA21, the self-assembled H1 for HCR on RCA formed nanoscaffold was opened, and then H2 probes for HCR can be swiftly opened to form whole DNAzyme structure. By cleaving the fluorescence quenched substrate probe, the fluorescence signal can be restored, and miRNA 21 can be sensitively detected. In the proposed assay, the RCA-based DNA nanoscaffold can be prepared in advance to save reaction time, and simple modification on the corresponding sequence of H1 probe in HCR can realize the detection of other miRNA targets without changing RCA nanoscaffold and DNAzyme sequence.

Materials and Method

Reagents and Materials

All the DNA sequences used in this study (Table 1) were synthesized by Sangon Biotech (Shanghai) Co., Ltd. (Shanghai, China). SplintR Ligase, phi29 DNA polymerase, and corresponding buffer were bought from New England Biolabs (Beijing, China). dNTPs were bought from Beijing Solarbio Science & Technology Co., Ltd. (Beijing, China). HEPES powder was purchased from Sigma-Aldrich (Shanghai, China). Unless otherwise indicated, all other chemical reagents were purchased from Sinopharm Chemical Reagent Co. Ltd. (Beijing, China). Solutions used in all experiments were obtained from ultra-pure water purified with a Milli-Q Water Purification System purchased from Merck Millipore (Billerica, MA, USA).

Construction of RCA-Based DNA Nanoscaffolds

The total RCA system was 10 μL included 0.2 μM lock probe and primer, 300 μM dNTP, 1.5 U SplintR ligase, 0.4 U phi29 DNA polymerase, and 0.5 μL of corresponding buffer, and the rest was supplemented with TE buffer. The reaction system was incubated at 37 °C for 1 h and then deactivated at 65 °C for 20 min. Two microliters (μL) of 10 μM of H1 probe was then added to the 10 μL of 20-fold diluted RCA product and was kept at room temperature

Table 1 DNA sequences used in this study

Probe	Target sequence (5′-3′)
MiRNA21	UAGCUUAUCAGACUGAUGUUGA [39]
H1	ATCAGACTGATGTTGAACTGACTCAACATCAGTCTGATAAGCTAAAAAAAA ACTCATACCATAT
H2	TCATTCAGCGATCCAAGTCAGTTCAACATCAGTCTGATTAGCTTATCAGACTGA TGTTGATTGGCACCCATGTACAGTC
Padlock Probe	P'ACCTCATCTCTCATACCATATAAATGCGCTAGGTATATAACCTCATACCATATT ATACAACCTACT
Primer	AGATGAGGTAGTAGGTTGTATA
Substrate Probe	FAM-TGACTG TTrAGGAATGAC-BHQ1 [38]
MiRNA Let7a	UGAGGUAGUAGGUUGUAUAGUU [39]
MiRNA133a	AGCUGGUAAAAUGGAACCAAAU [40]
MiRNA155	UUAAUGCUAAUCGUGAUAGGGGU [40]
One base-mismatched MiRNA21	UAGCUUAUCAGACUGAUGUUCA [39]

for 30 min. H1 probe was then fixed with the long ssDNA produced by RCA to form DNA nanoscaffolds. The finished product was kept at 4 °C for further use.

Target Triggered RNA-cleaving DNAzyme Reaction

To initiate the subsequent HCR reaction, 2 μL of a specific concentration of target miRNA21, 2 μL of 10 μM H2 probe, and 2 μL of 10 μM substrate probe were introduced to the previously constructed RCA-based DNA nanoscaffold. After a successful reaction, DNAzyme fragments modified at both ends of H2 formed a complete structure of DNAzyme, and cleaved the fluorescence-quenched substrate probe, which contained ribonucleobase (rA) and was labeled with the fluorophore/black hole quencher (FAM/BHQ-1) at the 5′ and 3′ end, respectively. The finished reaction system was filled with HEPES buffer (1 M NaCl, 20 mM $MgCl_2$, pH 7.4) to a final volume of 100 μL, and was transferred to a 96-well plate with a black translucent bottom for fluorescence intensity analysis (λex = 480 nm, λem = 520 nm) by multi-mode microplate readers (Cytation 3) (BioTek Instruments, Inc, Winooski, USA).

Data Analysis

Data analysis was performed using GraphPad software, and the results were reported as mean ± standard deviation (SD) from three separate experiments.

Results and Discussion

Principle of RCA-Based DNA Nanoscaffold Integrated with Target Triggered RNA-Cleaving DNAzyme Assay

The principle of RCA-based DNA nanoscaffold integrated with target triggered RNA-cleaving DNAzyme assay for sensitive detection of miRNA21 was shown in Fig. 1. Firstly, a long strand of ssDNA with hundreds or thousands of repeat units is formed by RCA reaction, and a sequence complementary to the end of H1 stem is designed at one end of the padlock probe. Then, H1 probe was added to bind with RCA products and DNA nanoscaffold was formed. More importantly, RCA-based DNA nanostructures can be prepared and stored in advance for further use.

In the presence of target miRNA, it hybridizes with the 3′ end of H1 probe, opens its original stem-loop structure, and exposes the sticky end. The exposed sticky end of H1 probe in turn hybridizes with the 3′ end of H2 probe and opens the stem-loop structure. After cycles of repeated ring-opening and hybridization, a large number of H1 and H2 probes alternately bind and extend into linear double-stranded DNA products. The process will lead to the rapid proximity of DNAzyme fragments modified at both ends of H2 probe to form a complete structure of DNAzyme. The formed intact DNAzyme captures fluorophore/black hole quencher (FAM/BHQ-1) labeled self-quenched substrate probe, cleaves

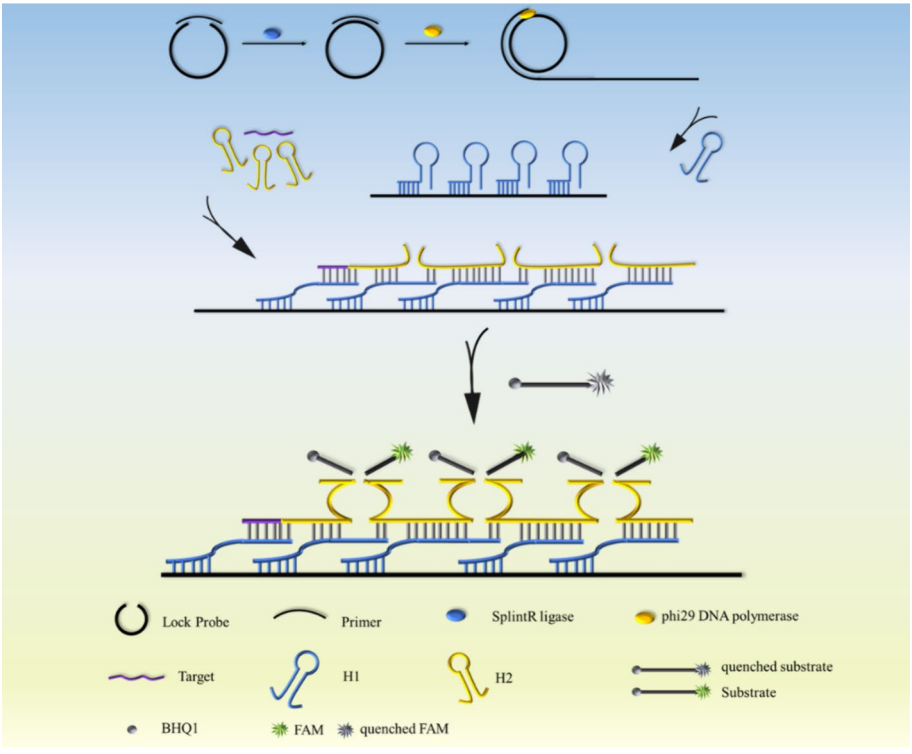

Fig. 1 The principle diagram of RCA-based DNA nanoscaffold integrated with target triggered RNA-cleaving DNAzyme assay

its central adenine ribonucleotide (rA), and the fluorescence is restored. By measuring the restored fluorescence intensity, target miRNA concentration can be sensitively detected. The proposed assay can realize the detection of other miRNA targets just needing modification on the corresponding sequence of H1 probe in HCR without any change on DNA nanoscaffold and DNAzyme sequence.

Optimization of Experimental Conditions

More and more experimental factor model designs have been developed, such as Box-Behnken Design (BBD) [39], Full Factorial Design (FFD) [40], Central Composite Design (CCD) [41], etc. Among them, CCD can evaluate the effects of individual factor and their interactions, reducing the numbers of tests. Thus, a single factor optimization strategy was adopted in the present study to optimize some important influencing factors on the construction of RCA-based DNA nanoscaffold and target triggered RNA-cleaving DNAzyme.

Optimization of the Conditions for RCA-Based DNA Nanoscaffold Formation

Previous studies showed that both the length and concentration of RCA products had a certain dependence on the reaction time [42, 43], thus the effect of RCA reaction time was evaluated. As shown in Fig. 2A, with the reaction time prolonging from 0.5 to1 h, the fluorescence intensity was enhanced. After this time point, the signal began to gradually weaken. One reason for this phenomenon might be that when the RCA product chain reaches a certain length, continued extension will increase the probability of arbitrary binding of H1 probe with RCA products, which is not conducive to the tight and orderly hybridization of H1 probe with H2 probe in HCR reaction, reduces the reaction efficiency, and finally weakens the fluorescence intensity. Another possible reason might be that with the reaction time increasing, the longer RCA product will self-assemble to form a certain adhesion structure [44, 45], which will sterically block the DNAzyme arranged on the upper edge of the formed DNA nanoscaffold, affects the cleavage efficiency of DNAzyme, and finally weakens the fluorescence intensity. Thus, 1 h was chosen as the optimal time for RCA reaction.

As previously mentioned, the RCA product contains hundreds or thousands of binding sites to H1 probe. If the amount of H1 probes is insufficient, continuing to open the structure of H1 probes by H2 probes is likely to be blocked. However, too many H1 probes may be free in solution and compete for H2 probes to undergo HCR reaction. Thus, the optimal ratio of the padlocked probe to H1 probe was needed to be investigated. The results were shown in Fig. 2B. With the ratio of padlock probe to H1 probe decreasing from 1:10 to 1:1000, the fluorescence intensity of the assay showed a tendency of increase and then decrease, and at the ration of 1:200, the highest fluorescence intensity can be obtained. Thus, 1:200 was chosen as the optimal ratio of padlock probe to H1 probe in the following experiment.

In addition, the ratio of H1 to H2 probe in HCR reaction was also optimized considering the signal output through the DNAzyme fragment at both ends of the adjacent H2 probe. From the results shown in Fig. 2C, it can be found that with the increase of the ratio of H1 probe to H2 probe from 1:1 to 4:1, the obtained fluorescence intensity was decreased. Thus, 1:1 was chosen as the optimal ratio of H1 probe to H2 probe, and was used in the following experiment.

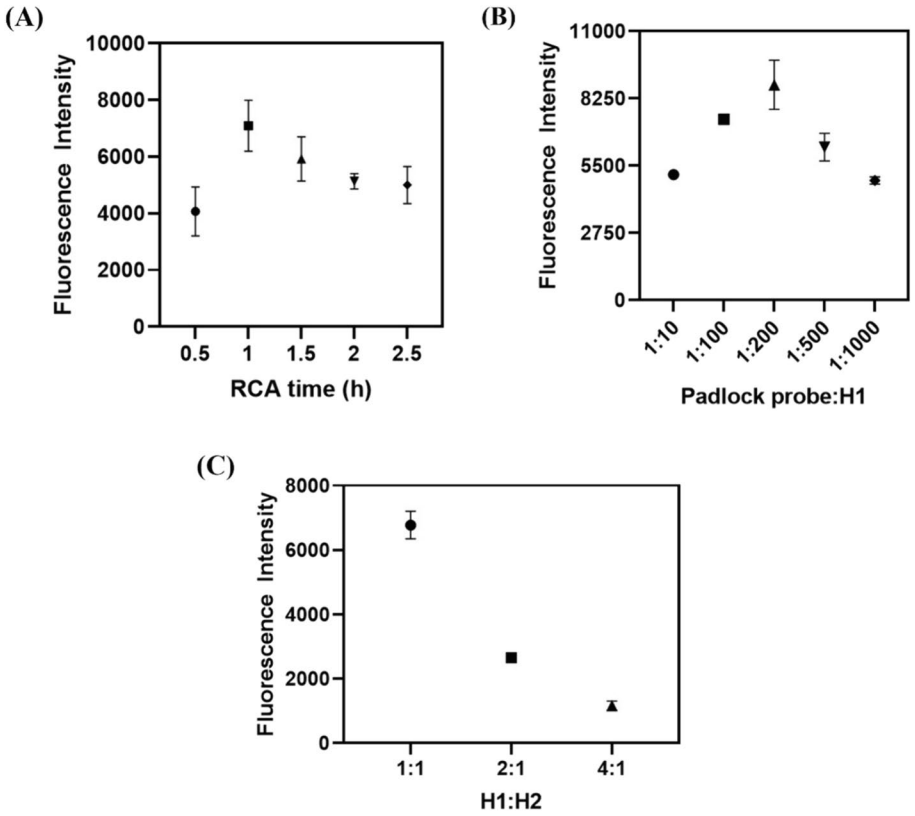

Fig. 2 Optimization of the conditions for RCA-based DNA nanoscaffold formation. **A** The effect of RCA reaction time on fluorescence signal intensity. **B** The effect of the ratio of padlock probe and H1 probe on fluorescence signal intensity. **C** The effect of the ratio of H1 probe and H2 probe on fluorescence signal intensity. Target miRNA21 concentration was 50 pM

Optimization of the Conditions for Target Triggered RNA-Cleaving DNAzyme

The factors that might affect the cleavage rate of DNAzymes were optimized herein, including the reaction temperature, cleavage time, substrate probe concentration, and magnesium ion (Mg^{2+}) concentration.

The effect of a series of temperature gradients from 15 to 50 °C on the detection was investigated, and the result was shown in Fig. 3A. It showed that with the temperature increasing from 15 to 25 °C, the fluorescence intensity was enhanced, which indicated that the hydrolysis rate of RNA phosphodiester bond by DNAzyme was accelerated. However, when the temperatures were higher than 25 °C, the obtained fluorescence intensity showed a decreasing tendency, indicating the reaction efficiency of DNAzyme was weakened. As we know, RNA cleaving DNAzyme is able to catalyze the deprotonation of 2′-OH (hydroxyl group at position 2 C) on ribose in the presence of metal ions, producing oxygenated anions, which in turn react with adjacent phosphate groups, resulting in phosphodiester bond hydrolysis of the RNA substrate, producing 2′, 3′ -cyclic phosphate and 5′ -OH groups, achieving the cleavage of the RNA substrate [46–48]. Although higher temperature

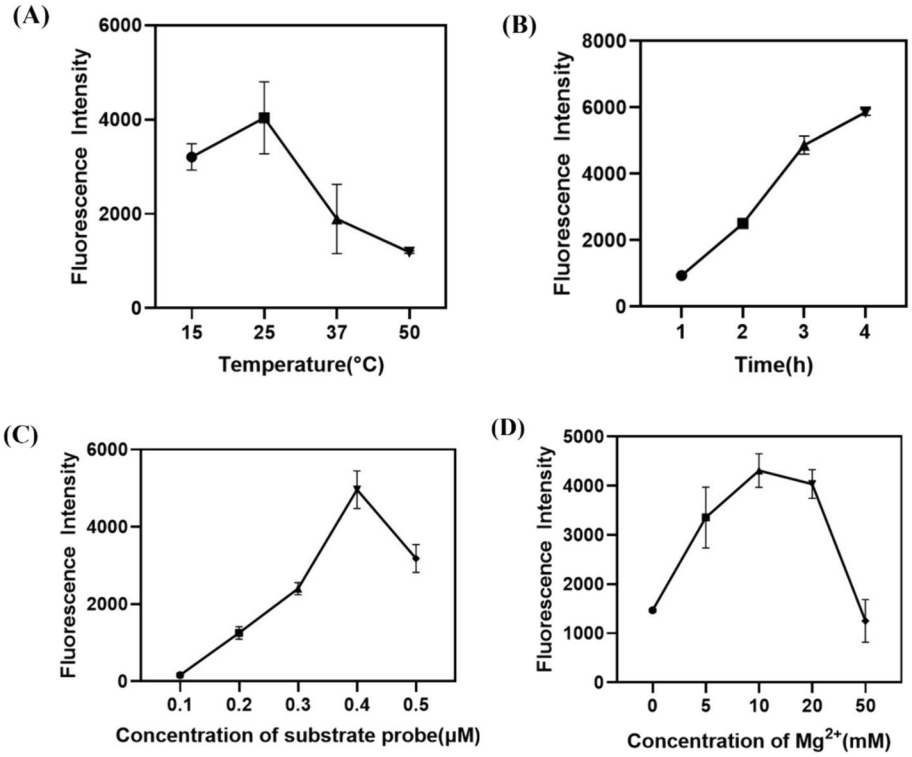

Fig. 3 Optimization of the conditions for target triggered RNA-cleaving DNAzyme activity. **A** The effect of reaction temperature on the activity of the formed RNA-cleaving DNAzyme. **B** The effect of reaction time on the activity of the formed RNA-cleaving DNAzyme. **C** The effect of substrate probe concentration on the activity of the formed RNA-cleaving DNAzyme. **D** The effect of Mg^{2+} concentration on the activity of the formed RNA-cleaving DNAzyme. Target miRNA21 concentration was 50 pM

can promote the collision frequency between molecules, the increased rate of phosphodiester hydrolysis counteracts the increased rate, thus affecting the cleavage efficiency of the overall reaction. Thus, 25 °C was chosen as the optimal reaction temperature, which was also a typical reaction temperature for HCR reaction [49–51].

The efficiency of DNAzymes is highly dependent on the cleavage time [38, 52, 53], so the effect of reaction time was investigated, and the results were shown in Fig. 3B. It can be seen that with the prolonging of the reaction time, the obtained fluorescence signal intensity showed an increasing tendency, but before 3 h, the increase level was faster, and after this time point, the increase level was tended to be slower. In order to save the whole reaction time, 3 h was chosen as the suitable reaction time for DNAzymes cleavage. The sensitivity and specificity of the proposed assay were partially guaranteed by the entire assembly of DNAzyme fragments and their cleavage activity. However, it might be noted that direct cleavage of self-assembly DNAzyme fragments sacrifices some reaction time when compared to the intact DNAzyme to some extent [52–54].

The concentration of the substrate probes was also optimized. As shown in Fig. 3C, with the increasing of the substrate probe concentration from 0.1 to 0.4 μM, the fluorescence intensity of the proposed assay was enhanced, but when the concentration was higher

than 0.4 μM, the fluorescence intensity decreased. The phenomenon might indicate that increasing the substrate probe concentration will allow DNAzyme to fully exhibit its cleaving activity and increase fluorescence signals; however, after reaching to a certain level, it will increase the background noise and reduce the signal-to-noise ratio. Thus, 0.4 μM was selected as the optimal substrate probe concentration.

Almost all the currently known DNAzymes rely on metal ions for cleavage [38, 55, 56]. Mg^{2+} are able to form metal ion-nucleic acid complex coordination structures with specific residues in the active site of the enzyme, such as acidic residues, thereby stabilizing the conformation of the enzyme and participating in intermediate steps of the catalytic reaction [57, 58]. Thus, the effect of different concentrations of Mg^{2+} on the cleavage of DNAzyme was investigated herein (Fig. 3D). The obtained results showed that with an increase of Mg^{2+} concentration from 0 to 50 mM, the fluorescence signal intensity showed a tendency of increase and then decrease, and the highest fluorescence intensity was obtained at Mg^{2+} concentration of 10 mM. In the presence of Mg^{2+} concentration higher than 10 mM, the fluorescence intensity decreased rapidly. The results indicated that too high concentrations of Mg^{2+} may interact with the negative charge in the structure of DNAzyme, resulting in the conformational changes or instability of DNAzyme, thereby weakening the binding to the substrate probe, and further reducing the catalytic activity. Thus, 10 mM was selected as the optimal Mg^{2+} concentration.

Analytical Performance of RCA-Based DNA Nanoscaffold Integrated with Target Triggered RNA-Cleaving DNAzyme Assay

Sensitivity of the Proposed Assay

Under the optimized experimental conditions, a gradient concentration of miRNA21 (1 pM to 100 pM) was detected by the proposed assay. The results shown in Fig. 4 indicated that with the increase of miRNA21 concentration, the intensity of fluorescence signal was enhanced, and a good linear relationship of $y = 2055x + 1691$ ($R^2 = 0.9589$) can be obtained between the fluorescence intensity and the logarithm of miRNA21 concentration ranging from 1 to 100 pM. According to the principle of 3σ, the detection limit was calculated to be 0.76 pM. The sensitivity of the proposed assay herein was super or comparable with that of other cascading methods as shown in Table 2.

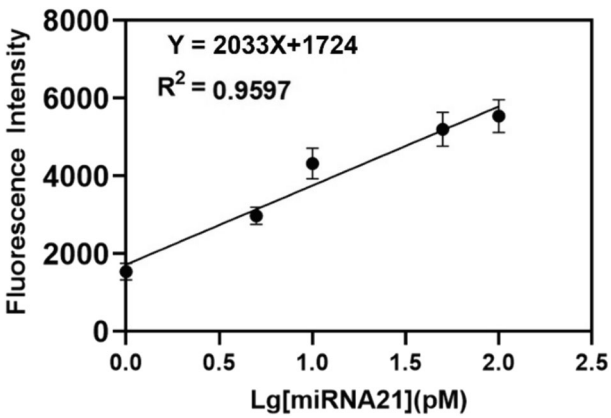

Fig. 4 The linear relationship between the fluorescence intensity and the logarithm of miRNA21 concentration

Table 2 Comparison of the analytical performance of different cascading amplification methods

Methodology	Target	Signal	LOD	Time	Reference
HCR-CHA	Standard DNA	Fluorescence	5 pM	16 h	[59]
CHA-HCR-DNAzyme	miRNA 21	Fluorescence	5 pM	4 h	[60]
CHA-RCD	mRNA	Fluorescence	9 pM	8 h	[61]
RCA-DNAzyme	miRNA 21	Fluorescence	4 pM	6 h	[62]
HCR-PMD	miRNA let-7a	Electrochemistry	1 pM	2 h	[63]
HCR-DNAzyme	HIV	Fluorescence	0.5 nM	80 min	[64]
CHA-HCR	Standard DNA	Fluorescence	5 pM	3.5 h	[65]
Cas13a-RCA	EV miRNA	Fluorescence	90 fM	3 h	[66]
RCA-based DNA Nanoscaffold and DNAzyme	miRNA 21	Fluorescence	0.76 pM	4 h	This work

Specificity of the Proposed Assay

In order to evaluate the specificity of the proposed assay, miRNA21, miRNA21 mismatched one base, miRNAlet-7a, miRNA133a, and miRNA155 at the concentration of 50 pM were used as targets for detection. The results shown in Fig. 5 indicated the fluorescence intensity of miRNA21 was high, but the fluorescence intensity of miRNAlet-7a,

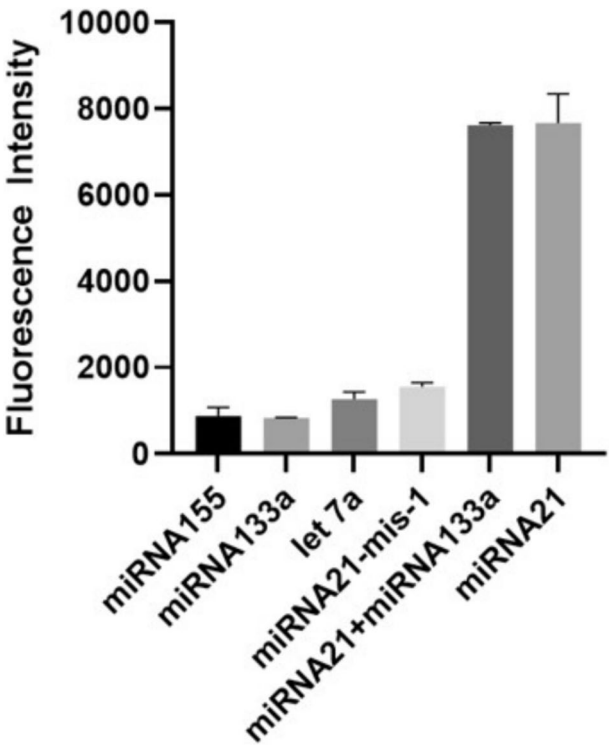

Fig. 5 Specificity evaluation of the proposed assay by detecting different miRNA

miRNA133a, miRNA155, and miRNA21 mismatched one base was very low, and was almost similar with that of the blank group. In addition, the mixture of miRNA21 and miRNA133a was also detected; the result showed that the fluorescence signal intensity of the mixture was almost equal to that of miRNA21 separately. All the obtained results demonstrated that the proposed assay based on RCA-based DNA nanoscaffold and target triggered DNAzyme was specific for miRNA21. The detection was not interfered by other nucleic acid sequences, and only one-base mismatched miRNA21 can also be effectively recognized.

Accuracy of the Proposed Assay

In order to evaluate the accuracy of the proposed assay, low (1 pM), medium (50 pM), and high concentration (100 pM) of miRNA21 were spiked in 20-fold diluted fetal bovine serum (FBS) and were detected. The recovery was calculated according to the found and the spiked concentration of miRNA21. The results were shown in Table 3. It can be found that the recoveries were ranged from 82.1 to 115.0%, and the coefficient of variation (CV) of intra-assay and inter-assay were ranged from 9.6 to 12.4% and 11.2 to 15.6%, respectively. All the results demonstrated that the proposed assay was accurate and precise. It further indicated the proposed assay was specific, and the serum matrix did not cause any interference for the detection. The proposed assay was suitable for sensitive miRNA 21 detection in serum.

Conclusions

Integration of RCA-based DNA nanoscaffold with target triggered RNA-cleaving DNAzyme, an assay for simple, specific, sensitive, accurate, and precise detection of miRNA21 was developed in the present study. Under the optimal conditions, 0.76 pM of miRNA21 can be detected, and only one-base mismatched miRNA21 can be effectively recognized. Other non-target miRNA and serum matrix did not cause any interference for miRNA21 detection.

Compared with other cascaded isothermal amplification techniques, RCA products were used as the DNA nanoscaffold, the immobilization of H1 probes on the RCA scaffold can increase the local concentration and significantly improve the reaction efficiency, while DNAzyme can cycle to produce a fluorescence signal under stable conditions. In addition, the proposed assay can realize the detection of other miRNA targets without changing the RCA nanoscaffold and DNAzyme sequence, just needing modification on the corresponding sequence of H1 probe in HCR. Moreover, in practical application, the RCA-based DNA nanoscaffold can be prepared in advance and stored for further use; once target miRNA, H2 probe, and substrate probe were added simultaneously, the HCR reaction on the

Table 3 The precision and accuracy of the proposed assay for detection of miRNA 21 spiked in fetal bovine serum

No	Spiked (pM)	Found (pM)	Recovery (%)	CV intra-assay (%)	CV inter-assay (%)
1	1	0.8	82.1	10.5	14.7
2	50	57.5	115.0	9.6	11.2
3	100	111.2	111.2	12.4	15.6

nanoscaffold will be triggered, which was convenient for rapid detection without complex operation. The integration of RCA-based DNA nanoscaffold with target triggered RNA-cleaving DNAzyme provides new ideas for more sensitive nucleic acid detection based on isothermal amplification techniques, which will play a vital role in clinical diagnosis.

Author Contribution Xuefei Lv conceived and designed the study. Yuan Li performed laboratory experiments. Yuan Li, Xuefei Lv, and Hao Jiang analyzed data and interpreted the results. Yuan Li and Xuefei Lv drafted, edited, and revised the manuscript. Xiaoqiong Li and Yulin Deng made modification on the manuscript. All authors approved the final version of the manuscript.

Funding This work was financially supported by National Key Research and Development Program of China (2022YFC2602900-03).

Data Availability The data sets utilized or analyzed in this study can be obtained from the corresponding author upon reasonable request.

Declarations

Ethics Approval Not applicable.

Consent to Participate Not applicable.

Consent for Publication Not applicable.

Conflict of Interest The authors declare no conflict of interest.

References

1. Millar, A. A., & Waterhouse, P. M. (2005). Plant and animal micrornas: Similarities and differences. *Functional & Integrative Genomics, 5*, 129–135.
2. Ikeda, S., Kong, S. W., Lu, J., Bisping, E., Zhang, H., Allen, P. D., Golub, T. R., Pieske, B., & Pu, W. T. (2007). Altered microrna expression in human heart disease. *Physiological Genomics, 31*, 367–373.
3. Sun, K., & Lai, E. C. (2013). Adult-specific functions of animal micrornas. *Nature Reviews Genetics, 14*, 535–548.
4. Bartel, D. P. (2009). Micrornas: Target recognition and regulatory functions. *Cell, 136*, 215–233.
5. Sayed, D., & Abdellatif, M. (2011). Micrornas in development and disease. *Physiological Reviews, 91*, 827–887.
6. Acharya, S. S., Fendler, W., Watson, J., Hamilton, A., Pan, Y., Gaudiano, E., et al. (2015). Serum micrornas are early indicators of survival after radiation-induced hematopoietic injury. *Science Translational Medicine, 7*, 269r–287r.
7. Yokoi, A., Matsuzaki, J., Yamamoto, Y., Yoneoka, Y., Takahashi, K., Shimizu, H., et al. (2018). Integrated extracellular microrna profiling for ovarian cancer screening. *Nature Communications, 9*, 4319.
8. Huang, R., He, L., Xia, Y., Xu, H., Liu, C., Xie, H., et al. (2019). A sensitive aptasensor based on a hemin/g-quadruplex-assisted signal amplification strategy for electrochemical detection of gastric cancer exosomes. *Small, 15*, e1900735.
9. Yu, S., Wang, Y., Jiang, L. P., Bi, S., & Zhu, J. J. (2018). Cascade amplification-mediated in situ hotspot assembly for microrna detection and molecular logic gate operations. *Analytical Chemistry, 90*, 4544–4551.
10. Shah, P., & Wang, Z. W. (2019). Using digital polymerase chain reaction to characterize microbial communities in wetland mesocosm soils under different vegetation and seasonal nutrient loadings. *Science of the Total Environment, 689*, 269–277.
11. Tison, A., & Saraux, A. (2019). Potential role for urine polymerase chain reaction in the diagnosis of whipple disease. *Clinical Infectious Diseases, 69*, 904–905.
12. Ali, K., Muller, T. H., Garritsen, H., Harringer, W., & Doescher, A. (2023). Digital polymerase chain reaction to monitor platelet transfusions in cardiac surgery patients. *Vox Sanguinis, 118*, 384–391.

13. Zhao, Y., Chen, F., Li, Q., Wang, L., & Fan, C. (2015). Isothermal amplification of nucleic acids. *Chemical Reviews, 115*, 12491–12545.
14. De Felice, M., De Falco, M., Zappi, D., Antonacci, A., & Scognamiglio, V. (2022). Isothermal amplification-assisted diagnostics for covid-19. *Biosensors and Bioelectronics, 205*, 114101.
15. Qi, H., Yue, S., Bi, S., Ding, C., & Song, W. (2018). Isothermal exponential amplification techniques: From basic principles to applications in electrochemical biosensors. *Biosensors & Bioelectronics, 110*, 207–217.
16. Wang, Y., Wang, D., Qi, G., Hu, P., Wang, E., & Jin, Y. (2023). Glass nanopipette-based plasmonic sers platform for single-cell microrna-21 sensing during apoptosis. *Analytical Chemistry, 95*, 16234–16242.
17. Yu, Y., Chen, Z., Jian, W., Sun, D., Zhang, B., Li, X., & Yao, M. (2015). Ultrasensitive electrochemical detection of avian influenza a (h7n9) virus dna based on isothermal exponential amplification coupled with hybridization chain reaction of dnazyme nanowires. *Biosensors & Bioelectronics, 64*, 566–571.
18. Chen, X., Huang, C., Nie, F., & Hu, M. (2023). Enzyme-free and sensitive method for single-stranded nucleic acid detection based on cha and hcr. *Analytical Methods, 15*, 4243–4251.
19. Xie, S., Chai, Y., Yuan, Y., Bai, L., & Yuan, R. (2014). A novel electrochemical aptasensor for highly sensitive detection of thrombin based on the autonomous assembly of hemin/g-quadruplex horseradish peroxidase-mimicking dnazyme nanowires. *Analytica Chimica Acta, 832*, 51–57.
20. Tian, W., Li, P., He, W., Liu, C., & Li, Z. (2019). Rolling circle extension-actuated loop-mediated isothermal amplification (rca-lamp) for ultrasensitive detection of micrornas. *Biosensors & Bioelectronics, 128*, 17–22.
21. Cheng, H., Li, W., Duan, S., Peng, J., Liu, J., Ma, W., Wang, H., He, X., & Wang, K. (2019). Mesoporous silica containers and programmed catalytic hairpin assembly/hybridization chain reaction based electrochemical sensing platform for microrna ultrasensitive detection with low background. *Analytical Chemistry, 91*, 10672–10678.
22. Xue, Y., Xie, H., Wang, Y., Feng, S., Sun, J., Huang, J., & Yang, X. (2022). Novel and sensitive electrochemical/fluorescent dual-mode biosensing platform based on the cascaded cyclic amplification of enzyme-free ddsa and functional nucleic acids. *Biosensors and Bioelectronics, 218*, 114762.
23. Huang, Y., Huang, X., Zheng, H., Lin, C., & Lin, Z. (2021). Homogeneous electrochemical biosensor for microrna based on enzyme-driven cascaded signal amplification strategy. *Analytical and Bioanalytical Chemistry, 413*, 4681–4688.
24. Xiang, J., Zhang, J., Li, S., Yuan, R., & Xiang, Y. (2022). Aptamer-based and sensitive label-free colorimetric sensing of phenylalanine via cascaded signal amplifications. *Analytica Chimica Acta, 1230*, 340393.
25 Liao, L., Li, X., Jiang, B., Zhou, W., Yuan, R., & Xiang, Y. (2022). Cascaded and nonlinear dna assembly amplification for sensitive and aptamer-based detection of kanamycin. *Analytica Chimica Acta, 1204*, 339730.
26. Qiu, Y., Dang, W., Fan, J., Zhou, T., Li, B., Liu, Y., et al. (2020). Dnazyme and rgo based fluorescence assay for fpg activity analysis, drug screening, and bacterial imaging. *Talanta, 218*, 121158.
27. Huang, X., Li, Z., Shi, Y., Zhang, Y., Shen, T., Chen, M., et al. (2023). A dnazyme dual-feedback autocatalytic exponential amplification biocircuit for microrna imaging in living cells. *Biosensors and Bioelectronics, 241*, 115669.
28. Li, X., Zhang, H., Tang, Y., Wu, P., Xu, S., & Zhang, X. (2017). A both-end blocked peroxidase-mimicking dnazyme for low-background chemiluminescent sensing of mirna. *ACS Sensors, 2*, 810–816.
29 Nie, K., Jiang, Y., Wang, N., Wang, Y., Li, D., Zhan, L., Huang, C., & Li, C. (2022). Programmable, universal dnazyme amplifier supporting pancreatic cancer-related mirnas detection. *Chemosensors, 10*, 276.
30. Chen, H. J., Hu, Y., Yao, P., Ning, D., Zhang, Y. P., Wang, Z. G., Liu, S. L., & Pang, D. W. (2021). Accurate and efficient lipoprotein detection based on the hcr-dnazyme platform. *Analytical Chemistry, 93*, 6128–6134.
31. Cheng, W., Yao, Y., Li, D., Duan, C., Wang, Z., & Xiang, Y. (2023). Asymmetrically split dnazyme-based colorimetric and electrochemical dual-modal biosensor for detection of breast cancer exosomal surface proteins. *Biosensors and Bioelectronics, 238*, 115552.
32. Du, M., Zheng, J., Tian, S., Liu, Y., Zheng, Z., Wang, H., Xia, J., Ji, X., & He, Z. (2021). Dnazyme walker for homogeneous detection of enterovirus ev71 and cvb3. *Analytical Chemistry, 93*, 5606–5611.
33. Chen, J., Wang, M., Zhou, C., Zhang, J., & Su, X. (2022). Label-free and dual-mode biosensor for hpv dna based on dna/silver nanoclusters and g-quadruplex/hemin dnazyme. *Talanta, 247*, 123554.
34. Davis, B. N., Hilyard, A. C., Lagna, G., & Hata, A. (2008). Smad proteins control drosha-mediated microrna maturation. *Nature, 454*, 56–61.

35. Li, T., Liang, Y., Li, J., Yu, Y., Xiao, M. M., Ni, W., Zhang, Z., & Zhang, G. J. (2021). Carbon nanotube field-effect transistor biosensor for ultrasensitive and label-free detection of breast cancer exosomal mirna21. *Analytical Chemistry, 93*, 15501–15507.
36. Wang, Y., Fang, Y., Zhu, Y., Bi, S., Liu, Y., & Ju, H. (2022). Single cell multi-mirnas quantification with hydrogel microbeads for liver cancer cell subtypes discrimination. *Chemical Science, 13*, 2062–2070.
37. Wang, J., Wang, D. X., Ma, J. Y., Wang, Y. X., & Kong, D. M. (2019). Three-dimensional dna nanostructures to improve the hyperbranched hybridization chain reaction. *Chemical Science, 10*, 9758–9767.
38. Wang, H., Li, C., Liu, X., Zhou, X., & Wang, F. (2018). Construction of an enzyme-free concatenated dna circuit for signal amplification and intracellular imaging. *Chemical Science, 9*, 5842–5849.
39. Shi, C. X., Li, S. X., Chen, Z. P., Liu, Q., & Yu, R. Q. (2019). Label-free and multiplexed quantification of micrornas by mass spectrometry based on duplex-specific-nuclease-assisted recycling amplification. *Analytical Chemistry, 91*, 2120–2127.
40. Ahmadi, M., Rahbarghazi, R., Shahbazfar, A. A., Baghban, H., & Keyhanmanesh, R. (2018). Bone marrow mesenchymal stem cells modified pathological changes and immunological responses in ovalbumin-induced asthmatic rats possibly by the modulation of mirna155 and mirna133. *General Physiology and Biophysics, 37*, 263–274.
41. Shokri, A. (2020). Using mn based on lightweight expanded clay aggregate (leca) as an original catalyst for the removal of no2 pollutant in aqueous environment. *Surfaces and Interfaces, 21*, 100705.
42. Shokri, A. (2022). Degradation of 4-chloro phenol in aqueous media thru uv/persulfate method by artificial neural network and full factorial design method. *International Journal of Environmental Analytical Chemistry, 102*, 5077–5091.
43. Shokri, A. (2022). Employing electro-peroxone process for degradation of acid red 88 in aqueous environment by central composite design: a new kinetic study and energy consumption. *Chemosphere, 296*, 133817.
44. Liu, D., Daubendiek, S. L., Zillman, M. A., Ryan, K., & Kool, E. T. (1996). Rolling circle dna synthesis: Small circular oligonucleotides as efficient templates for dna polymerases. *Journal of the American Chemical Society, 118*, 1587–1594.
45. Jonstrup, S. P., Koch, J., & Kjems, J. (2006). A microrna detection system based on padlock probes and rolling circle amplification. *RNA, 12*, 1747–1752.
46. Zhu, G., Hu, R., Zhao, Z., Chen, Z., Zhang, X., & Tan, W. (2013). Noncanonical self-assembly of multifunctional dna nanoflowers for biomedical applications. *Journal of the American Chemical Society, 135*, 16438–16445.
47. Hu, R., Zhang, X., Zhao, Z., Zhu, G., Chen, T., Fu, T., & Tan, W. (2014). Dna nanoflowers for multiplexed cellular imaging and traceable targeted drug delivery. *Angewandte Chemie International Edition in English, 53*, 5821–5826.
48. Wang, H., Wang, H., Wu, Q., Liang, M., Liu, X., & Wang, F. (2019). A dnazyme-amplified dna circuit for highly accurate microrna detection and intracellular imaging. *Chemical Science, 10*, 9597–9604.
49. Mcconnell, E. M., Cozma, I., Mou, Q., Brennan, J. D., Lu, Y., & Li, Y. (2021). Biosensing with dnazymes. *Chemical Society Reviews, 50*, 8954–8994.
50. Huang, Z., Wang, X., Wu, Z., & Jiang, J. H. (2022). Recent advances on DNAzyme-based sensing. *Chemistry - An Asian Journal, 17*, e202101414.
51. Gu, Y., Song, J., Li, M., Zhang, T., Zhao, W., Xu, J., Liu, M., & Chen, H. (2017). Ultrasensitive microrna assay via surface plasmon resonance responses of au@ag nanorods etching. *Analytical Chemistry, 89*, 10585–10591.
52. Qin, Y., Li, D., Yuan, R., & Xiang, Y. (2019). Netlike hybridization chain reaction assembly of dna nanostructures enables exceptional signal amplification for sensing trace cytokines. *Nanoscale, 11*, 16362–16367.
53. Prinzen, A. L., Saliba, D., Hennecker, C., Trinh, T., Mittermaier, A., & Sleiman, H. F. (2020). Amplified self-immolative release of small molecules by spatial isolation of reactive groups on dna-minimal architectures. *Angewandte Chemie International Edition, 59*, 12900–12908.
54. Wang, F., Elbaz, J., Orbach, R., Magen, N., & Willner, I. (2011). Amplified analysis of dna by the autonomous assembly of polymers consisting of dnazyme wires. *Journal of the American Chemical Society, 133*, 17149–17151.
55. Yang, H., Weng, B., Liu, S., Kang, N., Ran, J., Deng, Z., Wang, H., Yang, C., & Wang, F. (2022). Acid-improved dnazyme-based chemiluminescence mirna assay coupled with enzyme-free concatenated dna circuit. *Biosensors and Bioelectronics, 204*, 114060.

56. Xu, J., Qin, Y., Liang, Q., Zhong, X., Hou, L., Huang, Y., Zhao, S., & Liang, H. (2022). A mnox -nucleic acid nanoprobe with enzyme-free cascade signal amplification for ultrasensitive intracellular microrna imaging. *Chemical Communications, 58*, 12883–12886.
57. Mcghee, C. E., Loh, K. Y., & Lu, Y. (2017). Dnazyme sensors for detection of metal ions in the environment and imaging them in living cells. *Current Opinion in Biotechnology, 45*, 191–201.
58. Khan, S., Burciu, B., Filipe, C., Li, Y., Dellinger, K., & Didar, T. F. (2021). Dnazyme-based biosensors: Immobilization strategies, applications, and future prospective. *ACS Nano, 15*, 13943–13969.
59. Huang, Z., Wang, X., Wu, Z., Jiang, J. H. (2022). Recent advances on dnazyme-based sensing. *Chemistry – An Asian Journal, 17*(6), e202101414.
60. Russo, N., Toscano, M., & Grand, A. (2003). Gas-phase absolute Ca2+ and Mg2+ affinity for nucleic acid bases. A theoretical determination. *The Journal of Physical Chemistry A, 107*, 11533–11538.
61. Leonarski, F., D'Ascenzo, L., & Auffinger, P. (2017). Mg2+ ions: Do they bind to nucleobase nitrogens? *Nucleic Acids Research, 45*, 987–1004.
62. Li, B., Jiang, Y., Chen, X., & Ellington, A. D. (2012). Probing spatial organization of dna strands using enzyme-free hairpin assembly circuits. *Journal of the American Chemical Society, 134*, 13918–13921.
63. Li, J. J., Li, W. N., Du, W. F., Lv, M. M., Wu, Z. K., & Jiang, J. H. (2018). Target induced reconstruction of dnazymatic amplifier nanomachines in living cells for concurrent imaging and gene silencing. *Chemical Communications (Cambridge), 54*, 10626–10629.
64. Fang, C., Ouyang, P., Yang, Y., Qing, Y., Han, J., Shang, W., Chen, Y., Du, J. (2021). Mirna detection using a rolling circle amplification and rna-cutting allosteric deoxyribozyme dual signal amplification strategy. *Biosensors (Basel), 11,* 222.
65. Hou, T., Li, W., Liu, X., & Li, F. (2015). Label-free and enzyme-free homogeneous electrochemical biosensing strategy based on hybridization chain reaction: A facile, sensitive, and highly specific microrna assay. *Analytical Chemistry, 87*, 11368–11374.
66. Guo, Q., Chen, Y., Song, Z., Guo, L., Fu, F., & Chen, G. (2014). Label-free and enzyme-free sensitive fluorescent detection of human immunodeficiency virus deoxyribonucleic acid based on hybridization chain reaction. *Analytica Chimica Acta, 852*, 244–249.
67. Jiang, Y., Li, B., Chen, X., & Ellington, A. D. (2012). Coupling two different nucleic acid circuits in an enzyme-free amplifier. *Molecules, 17*, 13211–13220.
68. Wang, R., Zhao, X., Chen, X., Qiu, X., Qing, G., Zhang, H., et al. (2020). Rolling circular amplification (rca)-assisted crispr/cas9 cleavage (race) for highly specific detection of multiple extracellular vesicle micrornas. *Analytical Chemistry, 92*, 2176–2185.